

interesting to note that while peptide B displays considerable helical induction in the presence of Zn^{2+} , peptide A is Cd^{2+} selective and addition of Zn^{2+} has no effect on the helical content. In addition, helicity is independent of concentration of added NaF up to 250 mM for both peptide A (2.5 μ M in 5 mM sodium borate, pH 8.0) and peptide B (2.0 μ M in 5 mM sodium borate, pH 6.1). A and B show CD spectra independent of the peptide concentration in the presence and the absence of metal ions in the measured range of 0.5–70 μ M, consistent with intramolecular helical structures.¹¹ Nonligated metal coordination sites are most likely occupied by water molecules, and addition of external ligands such as 5-nitro-1,10-phenanthroline or mercaptoethanol does not affect the stability of the helical conformation.

Support for the metal ion complexation site comes from NMR studies. Both of the histidine 2-H and 4-H resonances in peptide B (2.5 mM in D_2O , pH 6.6) occurring at δ 7.87 and 7.74 and δ 6.89 and 6.87 show upfield shifts upon addition of Zn^{2+} to δ 7.75 and 7.71 and δ 6.87 and 6.67, respectively. Similar results are obtained for peptide A (2.5 mM in D_2O , pH 6.5) in the absence (δ 7.91 and 6.95) and the presence of Cd^{2+} (δ 7.71 and 6.91). Of the 17 backbone amide protons in peptide A (3.0 mM, $CdCl_2$ 0.3 M in H_2O , pH 5.1), 11 have been sequentially assigned by using COSY and NOESY spectra.¹² Interestingly, amide resonances for N-terminal amino acid residues exhibit $^3J_{HN\alpha} < 5$ Hz, which is further evidence that helical structure extends to the N-terminus.

The above studies indicate that unprecedented levels of helicity can be induced in short monomeric peptides by taking advantage of selective metal ion complexation. Detailed structural characterization of these peptides using 2-D NMR techniques is currently in progress. We are also utilizing unnatural amino acid side chains as potential ligands as well as studying the feasibility of stabilizing proteins by this approach.

Acknowledgment. We thank our colleagues R. Lerner, L. Walters, J. Dyson, P. Wright, B. Iverson, D. Hilvert, D. Rideout, C. Wong, and A. Satterthwait for helpful discussions and criticisms.

- (10) (a) Wilson, E. W.; Martin, R. B. *Inorg. Chem.* **1970**, *9*, 528. (b) Michailidis, M. S.; Martin, R. B. *J. Am. Chem. Soc.* **1969**, *91*, 4683.
 (11) (a) DeGrado, W. F.; Lear, J. D. *J. Am. Chem. Soc.* **1985**, *107*, 7684. (b) Ho, S. P.; DeGrado, W. F. *J. Am. Chem. Soc.* **1987**, *109*, 6751.
 (12) Dyson, H. J. Personal communication.

Solution Structure of $(PPh_2Me)_2Fe(CO)(\eta^2-C(O)Me)I$. Direct DNMR Evidence for a Facile Alkyl \leftrightarrow η^2 -Acyl Equilibrium

Chet Jablonski*

Department of Chemistry
 Memorial University of Newfoundland
 St. John's, Newfoundland A1B 3X7, Canada

Gianfranco Bellachioma, Giuseppe Cardaci, and
 Gustavo Reichenbach

Dipartimento di Chimica, Università di Perugia
 I-06100 Perugia, Italy
 Received May 8, 1989

Transition-metal oxophilicity^{1,2} and steric³⁻⁶ factors have emerged as crucial parameters which determine the relative

- (1) Fachinetti, G.; Floriani, C.; Stoeckli-Evans, H. *J. Chem. Soc., Dalton Trans.* **1977**, 2297-2302. Curtis, M. D.; Shiu, K.-B.; Butler, W. M. *Organometallics* **1983**, *2*, 1475-1477. Moly, K. G. T.; Marks, T. J. *J. Am. Chem. Soc.* **1984**, *106*, 7051-7064. Carmona, E.; Sánchez, L.; Main, J. M.; Poveda, M. L.; Atwood, J. L.; Priester, R. D.; Rogers, R. D. *J. Am. Chem. Soc.* **1984**, *106*, 3214-3222. Hofmann, P.; Stauffert, P.; Tatsumi, K.; Nakamura, A.; Hoffman, R. *Organometallics* **1985**, *4*, 404-406. Curtis, M. D.; Shiu, K.-B.; Butler, W. M. *J. Am. Chem. Soc.* **1986**, *108*, 1550-1561. Kreissel, F. R.; Sieber, W. J.; Keller, H.; Riede, J.; Wolfigruber, M. *J. Organomet. Chem.* **1987**, *320*, 83-90. Rappe, A. K. *J. Am. Chem. Soc.* **1987**, *109*, 5605-5613. De Boer, E. J. M.; De With, J. J. *Organomet. Chem.* **1987**, *320*, 289-293. Onyiriuka, E. C.; Storr, A. *Can. J. Chem.* **1987**, *65*, 2464-2468.

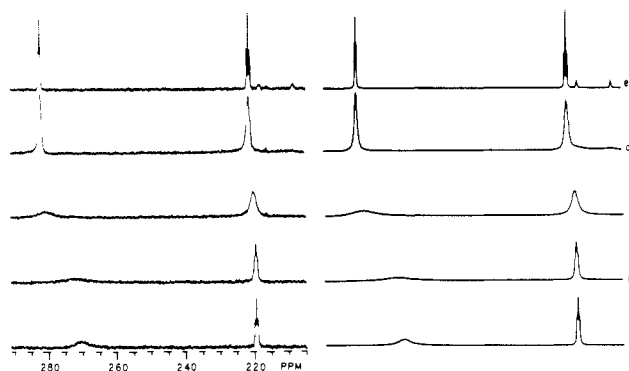
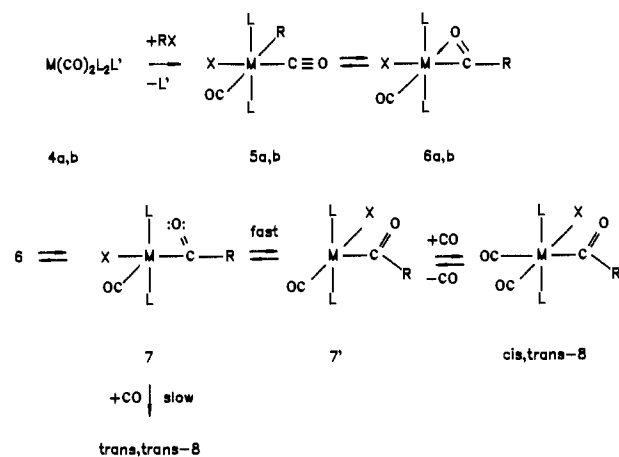


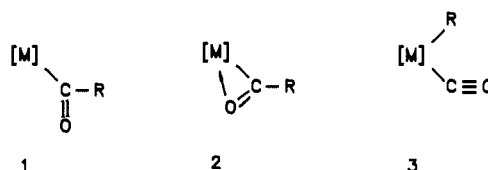
Figure 1. Variable-temperature ^{13}C NMR spectra in CD_2Cl_2 and DNMR simulations for $5b \leftrightarrow 6b$: a, 309.5 K; b, 296.8 K; c, 270.0 K; d, 244.6 K; e, 220.0 K.

Scheme 1^a



^a a: L = L' = PPh_3 , M = Ru, R = Me.¹³ b: L = PPh_2Me , L' = $MeCN^4$ or N_2 ,⁶ M = Fe, R = Me.

stability of mono- and bidentate acyl coordination modes 1 and 2 respectively. Although coordinatively saturated bidentate acyl



structures have been implicated as intermediates in CO insertion chemistry,⁷⁻¹² little direct evidence¹³ exists regarding the relative

- (2) Durfee, L. D.; Rothwell, I. P. *Chem. Rev.* **1988**, *88*, 1059-1079.
 (3) Sheeran, D. J.; Arenivar, J. D.; Orchin, M. *J. Organomet. Chem.* **1986**, *316*, 139-146.
 (4) Cardaci, G.; Bellachioma, G.; Zanazzi, P. *Organometallics* **1988**, *7*, 172-180. Cardaci, G.; Bellachioma, G. *Gazz. Chim. Ital.* **1986**, *116*, 475. Cardaci, G.; Bellachioma, G.; Reichenbach, G. *Int. Conf. Organomet. Chem., 12th, Vienna 1985*, 429.
 (5) Hermes, A. R.; Girolami, G. S. *Organometallics* **1988**, *7*, 394-401.
 (6) Birk, R.; Berke, H.; Huttner, G.; Zsolnai, L. *J. Organomet. Chem.* **1986**, *309*, C18-C20. Birk, R.; Berke, H.; Huttner, G.; Zsolnai, L. *Chem. Ber.* **1988**, *121*, 1557-1564.
 (7) Brunner, H.; Vogt, H. *Chem. Ber.* **1981**, *114*, 2186-2207.
 (8) Brunner, H.; Hammer, B.; Bernal, I.; Draux, M. *Organometallics* **1983**, *2*, 1595-1603.
 (9) Sweany, R. L. *Organometallics* **1989**, *8*, 175-179.
 (10) Shaver, A.; Quinn, S. *J. Am. Chem. Soc.* **1982**, *104*, 1096-1099.
 (11) Flood, T. C.; Campbell, K. D. *J. Am. Chem. Soc.* **1984**, *106*, 2853-2860.
 (12) Bidentate acyls may also play an important role in cis labilization; cf.: Ford, P. C.; Rokicki, A. *Adv. Organomet. Chem.* **1988**, *28*, 139-217.
 (13) In an early, insightful analysis of the solution IR spectra, Roper proposed that $5a$ and $6a$ (M = Ru, L = L' = PPh_3 , R = Me) were in rapid equilibrium in solution; cf.: Roper, W. R.; Taylor, G. E.; Waters, J. M.; Wright, L. J. *J. Organomet. Chem.* **1979**, *182*, C46-C48.

Table I. Kinetic and Thermodynamic Parameters for **5b** ↔ **6b**

temp, ^a K	k_{exch}^b , s ⁻¹	k_f , s ⁻¹	k_r , s ⁻¹	K_{eq}
220.0 ± 0.3	≤ 1.0	(1.7 ± 0.9) × 10 ³	(2.6 ± 1.9) × 10 ²	9.0 ± 1 ^c
244.6 ± 0.3	(1.0 ± 0.5) × 10 ³	(1.6 ± 0.4) × 10 ⁴	(3.2 ± 0.8) × 10 ³	6.6 ± 1.8 ^d
270.0 ± 0.3	(9.5 ± 2) × 10 ³	(8.8 ± 0.3) × 10 ⁴	(2.2 ± 0.7) × 10 ⁴	5.0 ± 1.4 ^d
296.8 ± 0.3	(5.5 ± 1.5) × 10 ⁴			4.1 ± 1 ^d
309.5 ± 0.3	≥ 7.5 × 10 ⁴			3.8 ± 0.7 ^e

^a Calibrated by using methanol or ethylene glycol standards. ^b Calculated from manual line-shape fits using DNMR-3H.¹⁹ ^c Determined by integration. ^d Calculated by using $\Delta H = -5.4 \pm 0.8$ kJ mol⁻¹, $\Delta S = -6.5 \pm 2$ J mol⁻¹ K⁻¹, obtained from data at 220 K and 309 K (cf. text). ^e Determined from weighted average chemical shift data of **6b** and **5b**.

stabilities and reaction dynamics connecting the bidentate acyl structure **2** with its isomeric parent alkyl **3**. Herein we report variable-temperature DNMR evidence which unequivocally demonstrates a facile alkyl ↔ η^2 -acyl migratory insertion/deinsertion **3** ↔ **2** and defines their relative thermodynamic and kinetic stabilities.

Oxidative addition of alkyl halides to "dissociatively activated" d⁸ Ru¹³ (**4a**) and Fe^{4,6} (**4b**) substrates proceeds readily even when the ligand sphere is sterically demanding (Scheme I). In contrast with oxidative addition to less hindered d⁸ substrates,¹⁴ structural evidence^{4,6} shows that the isolated product in these cases is a bidentate acyl, **6**, rather than a six-coordinate octahedral alkyl, **5**, respectively. Clearly a delicate balance exists between the isomeric alkyl and bidentate acyl structures, with increasing steric demands favoring the latter.^{4,6}

Examination of the ¹³C NMR spectrum¹⁵ of the bidentate acyl **6b** (M = Fe, L = PPh₂Me, R = Me) in dichloromethane-*d*₂ reveals that its solution structure differs markedly from that observed in the solid state.⁴ At ambient temperature, the phosphine methyls as well as the diastereotopic P(C₆H₅)₂ groups appear as sharp triplets, virtually coupled to two isochronous, trans ³¹P atoms. At the same temperature, however, the signals for the carbonyl and especially the acyl methyl are curiously broad. Furthermore, no resonance appropriate to the bidentate acyl carbon was detected at ambient temperature (293 K). These ambiguities were resolved by recording the ¹³C NMR spectrum of isotopically enriched **6b** at low temperature. Figure 1 shows partial, temperature-dependent ¹³C DNMR spectra recorded for a sample of **6b** specifically enriched at FeC*O and Fe(C*(O)CH₃).¹⁶ A rather large solubility temperature coefficient of **6b** in dichloromethane restricted the low-temperature limit to 203 K.¹⁷ On cooling, the broad carbonyl resonances at 270.0 and 220.0 ppm resolve into sharper signals at 282.3, 221.4, 218.2, and 208.5 ppm,¹⁸ cf. Figure 1. The observed changes are completely reversible. We interpret the variable-temperature ¹³C NMR spectra of Figure 1 in terms of the rapid equilibrium OCFeMe ↔ η^2 -FeC(O)Me, **5b** ↔ **6b**. The intense resonances at 282.3 and 221.4 ppm can be assigned to the acyl and carbonyl groups, respectively, for the bidentate

acyl isomer, **6b**.⁴ Low-intensity carbonyl resonances at 218.2 and 208.5 ppm are assigned to a smaller equilibrium concentration of the isomeric alkyl complex **5b**.

Equilibrium constants (cf. Table I) for **5b** ↔ **6b** were obtained by integration of the low-temperature-limiting ¹³C NMR spectrum (203 K) and from DNMR-3H¹⁹ fits at the high-temperature limit (309.5 K) in CD₂Cl₂. The enthalpy change, ΔH , for **5b** → **6b** was determined to be -5.4 kJ mol⁻¹, indicating that the bidentate acyl is only slightly more stable than its alkyl isomer. The low-temperature-limiting spectrum shows two, nonisochronous carbonyl triplets ($\delta = 218.2$ ppm ($J = 20.8$), 208.5 ppm ($J = 16.2$)), which can be confidently assigned²⁰ to the carbonyls trans to I and trans to Me, respectively, for the cis structure **5b**. ¹³C magnetization transfer experiments at 223 K demonstrated that the acyl site of **6b** specifically exchanged with the 218.2 ppm CO site of **5b**, which is, vide supra, cis to the methyl group. Consistent with these results is the observation that the diastereotopic *o*-C₆H₅ resonances are not averaged even at the fast-exchange limit. Thus, if the phosphorus ligands remain mutually trans, the insertion cannot pass through any intermediate having an axial symmetry plane.

Line-shape calculations¹⁹ of the exchanged-broadened ¹³C NMR spectra incorporated the specific site exchange of eq 1 demonstrated by magnetization transfer and allowed for the temperature dependence of the equilibrium constant. Good fits of the experimental data were then obtained by using the exchange rate as the only variable (cf. Figure 1). The temperature dependence of the ¹³C DNMR exchange rates established activation parameters, $\Delta H^\ddagger = 41.9 \pm 4$ kJ mol⁻¹ and $\Delta S^\ddagger = -28 \pm 15$ J mol⁻¹ K⁻¹, for the insertion (cf. Table I).

At 211 K, the bidentate acyl **6b** rapidly and quantitatively coordinates carbon monoxide to give the monodentate acyl *cis*,*trans*-Fe(CO)₂(PPh₂Me)₂(C(O)Me)I (**8**), which slowly isomerizes to afford *trans,trans*-**8** as the sole thermodynamic product. Similar stereochemical results have been reported for the carbonylation of other related *cis,trans*-Fe(CO)₂L₂(Me)X^{6,20,21} alkyls and bidentate acyls.⁶ Although a bimolecular mechanism involving back-side attack of CO concerted with η^2 -acyl → η^1 -acyl interconversion can in principle account for the observed stereochemistry, we believe that a dissociative mechanism is more likely. Opening of the bidentate acyl **6b** gives the 16e⁻ η^1 -acyl intermediate **7**, which is to some degree "protected" from external nucleophilic attack at the vacant site by the adjacent acyl oxygen. Thus **7** is not intercepted by CO and facile isomerization occurs, affording an "unprotected" 16e⁻ intermediate **7'** with apical acyl. Intermediate **7'** rapidly captures CO to give the observed *cis,trans* kinetic product.²² We note here that exchange of the R and O positions via rotation of the monodentate acyl-metal bond in **7** followed by alkyl migration provides a stereospecific route to **5b**.

If we accept the proposal that coordination of an external ligand by the η^2 -acyl is not concerted but rather a two-step process, our results imply that although coordinatively saturated bidentate acyls

(14) Pankowski, M.; Bigorgne, M. *J. Organomet. Chem.* **1983**, *251*, 333-338.

(15) The 60-MHz ¹H NMR spectrum of **6b** has been reported; cf. ref 4. We have reexamined the ¹H NMR spectrum at 300 MHz at ambient temperature and find that while the gross features remain, the resonance assigned to η^2 -C(O)CH₃ is a slightly broadened triplet.

(16) Unlabeled **6b** was prepared by using the method of Cardaci et al.; cf. ref 4. The specifically enriched **6b** used in this study was prepared from labeled (PPh₂Me)₂Fe(C*O)₃ by using a modification of the photochemical procedure reported by Berke; cf. ref 6. Its structure was verified by comparison of ¹H and ¹³C NMR spectra with those determined from an authentic sample.

(17) The low-temperature solubility of **6b** is appreciably greater in THF. At 203 K, both carbonyl resonances were well-resolved triplets. Similar dynamic behavior occurred on warming.

(18) **6b**: 75-MHz ¹³C{¹H} NMR (CD₂Cl₂, 220 K) δ C(O)Me, 282.3 (t, $J = 17.3$); CO, 221.4 (t, $J = 38.0$); *ipso*-C₆H₅, 136.4 (t, $J = 23.1$), 135.4 (t, $J = 24.7$); *o*-, *m*-C₆H₅, 133.9 (t), 131.7 (t), 130.7 (t), 130.2 (t); *p*-C₆H₅, 128.7 (m); C(O)Me, 13.5 (t, $J = 14$); PMe, 13.6 (t, $J = 14.0$). **5b**: 75-MHz ¹³C{¹H} NMR (CD₂Cl₂, 220 K) δ CO, 218.2 (t, $J = 20.8$), 208.5 (t, $J = 16.2$); C₆H₅, 135.1 (t, $J = 21.4$), 133.1, 130.5, 130.5; PMe, 18.1 (t, 16.5). The ¹³C NMR spectrum of specifically labeled **6b** was identical except for intensity increases of the carbonyl resonances; cf. Figure 1. The chemical shifts reported for the carbonyl groups of **5b** were measured by using an enriched sample. Coupling constants reported for the carbonyl resonances of **5b** were determined in THF-*d*₆ at 203 K.

(19) Binsch, G.; Kleier, D. A.; Stempfle, W.; Klein, J.; Hoffmann, E. G. "DNMR3H: General Line-Shape Program with Symmetry and Magnetic Equivalence Factoring"; Program 450, Quantum Chemistry Program Exchange, Indiana University, 1982. Jackman, L. M.; Cotton, F. A., Eds. *Dynamic Nuclear Magnetic Resonance Spectroscopy*; Academic Press: New York, 1975.

(20) Wright, S. C.; Baird, M. C. *J. Am. Chem. Soc.* **1985**, *107*, 6899-6902.

(21) Cardaci, G.; Reichenbach, G.; Bellachioma, G. *Inorg. Chem.* **1984**, *23*, 2936-2940.

(22) Isotopic labeling studies to test this point are currently underway.

are both thermodynamically and kinetically accessible from their isomeric alkyl structures, they are not *required* intermediates in CO insertion chemistry. Bidentate acyl coordination reversibly traps the intermediate, producing an observable species in sterically congested systems.²³ Reversion to a monodentate coordination mode precedes conversion to the six-coordinate product in a manner analogous to the "dissociative trapping" mechanism demonstrated by Halpern²⁴ for nucleophilic catalysis of migratory CO insertion.

Acknowledgment. This work was supported by grants from the NATO Collaborative Research Grants Programme (Grant 86/337), the Natural Science and Engineering Council of Canada (NSERC), and the Consiglio Nazionale della Ricerche (CNR, Rome).

(23) We thank a referee for pointing out that other factors such as solvation may also be important in determining the position of the methyl \leftrightarrow η^2 -acyl equilibrium, particularly when the energy change is very small. Examination of **6b** in THF shows that the equilibrium is shifted significantly toward the alkyl isomer **5b** compared to methylene chloride.

(24) Webb, S. L.; Giandomenico, C. M.; Halpern, J. *J. Am. Chem. Soc.* **1986**, *108*, 345-347.

Structural Consequences of Nickel versus Macrocycle Reductions in F430 Models: EXAFS Studies of a Ni(I) Anion and Ni(II) π Anion Radicals

Lars R. Furenlid,^{1a} Mark W. Renner,^{1a} Kevin M. Smith,^{1b} and Jack Fajer*,^{1a}

Department of Applied Science
Brookhaven National Laboratory
Upton, New York 11973

Department of Chemistry, University of California
Davis, California 95616

Received September 11, 1989

Factor 430 (F430) is a nickel tetrapyrrole (hydrocorphin) found in methyl coenzyme M reductase, the enzyme that catalyzes the final stages of the reduction of carbon dioxide to methane in methanogenic bacteria.² Detection of EPR signals attributable to Ni(I) in the catalytic cycle of *Methanobacterium thermoautotrophicum*³ has led to intensive investigations of the reductive chemistry of F430 and of nickel porphyrins and hydrophyrins.⁴⁻⁸ Reduction of Ni(II) F430⁴ and isobacteriochlorins^{5,6} unambiguously results in Ni(I) species whereas porphyrins,⁵⁻⁹ chlorins,^{5,6} and hexahydro- and octahydro-porphyrins⁶ yield anions variously ascribed to Ni(I) or Ni(II) π radicals with some metal character.

The structural consequences associated with the reduction of Ni(II) to Ni(I) in porphyrin derivatives are unknown.⁹ Changes

(1) (a) Brookhaven National Laboratory. (b) University of California, Davis.

(2) Ellefson, W. L.; Whitman, W. B.; Wolfe, R. S. *Proc. Natl. Acad. Sci. U.S.A.* **1982**, *79*, 3707. Hausinger, R. P.; Orme-Johnson, W. H.; Walsh, C. *Biochemistry* **1984**, *23*, 801. Daniels, L.; Sparling, R.; Sprout, G. D. *Biochim. Biophys. Acta* **1984**, *768*, 113. Fässler, A.; Kobelt, A.; Pfaltz, A.; Eschenmoser, A.; Bladon, C.; Battersby, A. R.; Thauer, R. K. *Helv. Chim. Acta* **1985**, *68*, 2287 and references therein.

(3) Albracht, S. P. J.; Ankel-Fuchs, D.; Van der Zwaan, J. W.; Fontijn, R. D.; Thauer, R. K. *Biochim. Biophys. Acta* **1986**, *870*, 50. Albracht, S. P. J.; Ankel-Fuchs, D.; Böcher, R.; Ellerman, J.; Moll, J.; Van der Zwaan, J. W.; Thauer, R. K. *Biochim. Biophys. Acta* **1988**, *955*, 86.

(4) Jaun, B.; Pfaltz, A. *J. Chem. Soc., Chem. Commun.* **1986**, 1327.

(5) Stolzenberg, A. M.; Stershic, M. T. *Inorg. Chem.* **1987**, *26*, 1970; *J. Am. Chem. Soc.* **1988**, *110*, 6391 and references therein.

(6) Renner, M. W.; Forman, A.; Fajer, J.; Simpson, D.; Smith, K. M.; Barkigia, K. M. *Biophys. J.* **1988**, *53*, 277.

(7) Lexa, D.; Momenteau, M.; Mispelter, J.; Saveant, J. M. *Inorg. Chem.* **1989**, *28*, 30.

(8) Kadish, K. M.; Sazou, D.; Maiya, G. B.; Han, B. C.; Liu, Y. M.; Saoiabi, A.; Ferhat, M.; Guillard, R. *Inorg. Chem.* **1989**, *28*, 2542.

(9) Ni(I) and high spin Ni(II) thiaporphyrins have been reported recently: Latos-Grazynski, L.; Olmstead, M. M.; Balch, A. L. *Inorg. Chem.* **1989**, *28*, 4066. However, comparison with porphyrins is complicated by the sulfur ligated to Ni.

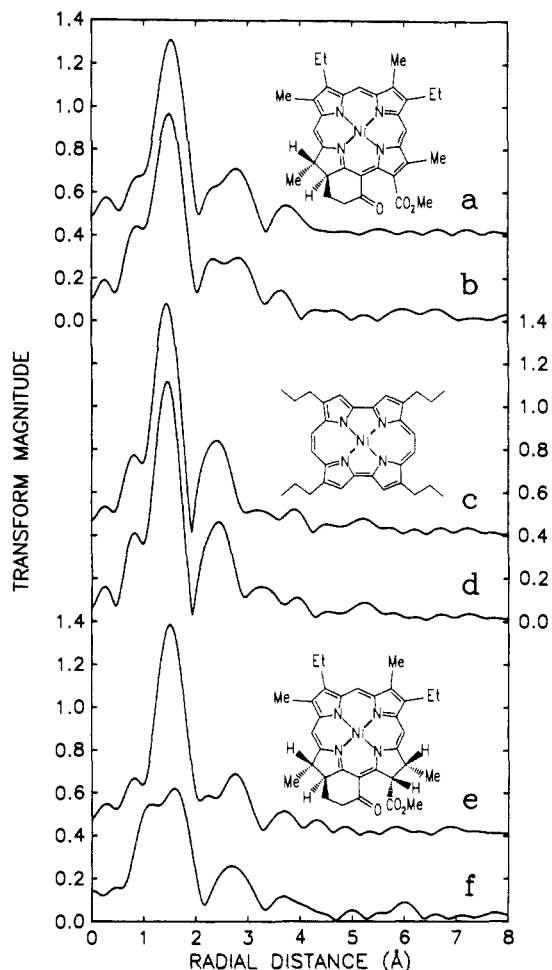


Figure 1. Chemical structures and Fourier transforms of k^2 weighted EXAFS oscillations for (a) Ni(II) chlorin, (b) Ni(II) chlorin π anion radical, (c) Ni(II) porphycene, (d) Ni(II) porphycene π anion radical, (e) Ni(II) iBC, and (f) Ni(I) iBC anion. Comparable spectra are offset for clarity (in THF; Bu_4N^+ is the counterion in all reduced species; $T = 298$ K).

as large as 0.2 Å in Ni-N distances have been suggested by Stolzenberg and Stershic for isobacteriochlorins.⁵ They and Renner et al.⁶ further suggested that, in addition to the relative ordering of the Ni(II) and π^* orbitals, the ability of the macrocycle to accommodate the larger Ni(I) controlled the sites of reduction, i.e., Ni(I) versus π anion radical.

We present here EXAFS results for the Ni(II) radical anions of a chlorin and a porphycene and for the Ni(I) anion of an isobacteriochlorin (iBC) that clearly demonstrate the structural consequences of metal versus macrocycle reductions.

Low-spin Ni(II) chlorin,¹⁰ porphycene¹¹ and iBC¹⁰ (see Figure 1 for structures) undergo reversible one-electron electrochemical reductions in tetrahydrofuran^{6,11} ($E_{1/2} = -1.04$, -0.80 , and -1.33 V, respectively, in the presence of 0.1 M $(\text{Bu})_4\text{NClO}_4$ vs SCE). Upon reduction, the chlorin and the porphycene exhibit optical spectra diagnostic of π anion radicals: loss of the visible bands and the appearance of weak broad bands stretching into the near infrared region.^{6,11-13} In frozen THF, at 115 K, the reduced species display EPR spectra typical of free radicals^{6,11,13} (the chlorin spectrum includes a shoulder on the high-field side,^{6,13} also noted by Kadish et al.⁸ for the π anion of a Ni porphyrin, sug-

(10) Chlorin: anhydrosorhodochlorin XV methyl ester. iBC: ring C of the chlorin also saturated. Smith, K. M.; Simpson, D. J. *J. Am. Chem. Soc.* **1987**, *109*, 6326.

(11) Porphycene: 2,7,12,17-tetrapropylporphycene. Renner, M. W.; Forman, A.; Wu, W.; Chang, C. K.; Fajer, J. *J. Am. Chem. Soc.* **1989**, *111*, 8618.

(12) Fujita, I.; Davis, M. S.; Fajer, J. *J. Am. Chem. Soc.* **1978**, *100*, 6280.

(13) Data are included in the supplementary material.